J Physiol (2003), **552.1**, *pp.* 185–195
DOI: 10.1113/jphysiol.2003.046904

www.jphysiol.org

Journal of Physiology

Role of elastin in spontaneously hypertensive rat small mesenteric artery remodelling

Ana M. Briones *, José M. González, Beatriz Somoza, Jesús Giraldo †, Craig J. Daly ‡, Elisabet Vila *, M. Carmen González, John C. McGrath † and Silvia M. Arribas

*Departamento de Fisiología, Facultad de Medicina, Universidad Autónoma de Madrid, Spain, * Departament de Farmacologia, de Terapèutica i de Toxicologia and † Grup de Modelització Estructural i Funcional de Sistemes Biològics, Facultat de Medicina, Universitat Autònoma de Barcelona, Spain and ‡ Autonomic Physiology Unit, University of Glasgow, Glasgow, UK*

Chronic hypertension is associated with resistance artery remodelling and mechanical alterations. However, the contribution of elastin has not been thoroughly studied. Our objective was to evaluate the role of elastin in vascular remodelling of mesenteric resistance arteries (MRA) from spontaneously hypertensive rats (SHR). MRA segments from Wistar Kyoto rats (WKY) and SHR were pressurised under passive conditions at a range of physiological pressures with pressure myography. Confocal microscopy was used to determine differences in the quantity and organisation of elastin in intact pressure-fixed arteries. To assess the contribution of elastin to MRA structure and mechanics, myograph-mounted vessels were studied before and after elastase incubation. When compared with WKY, MRA from SHR showed: (1) a smaller lumen, (2) decreased distensibility at low pressures, (3) a leftward shift of the stress–strain relationship, (4) redistribution of elastin within the internal elastic lamina (IEL) leading to smaller fenestrae but no change in fenestrae number or elastin amount. Elastase incubation (1) fragmented the structure of IEL in a concentration-dependent fashion, (2) abolished all the structural and mechanical differences between strains, and (3) decreased distensibility at low pressures. The study shows the overriding role of elastin in determining vascular dimensions and mechanical properties in a resistance artery. In addition, it informs hypertensive remodelling. MRA remodelling and increased stiffness are accompanied by elastin restructuring within the IEL and elastin degradation reverses structural and mechanical alterations of SHR MRA. Differences in elastin organisation are, therefore, a central element in small artery remodelling in hypertension.

(Resubmitted 19 May 2003; accepted after revision 4 July 2003; first published online 4 July 2003)
Corresponding author S. M. Arribas: Departamento de Fisiología, Facultad de Medicina, Universidad Autónoma de Madrid, C/ Arzobispo Morcillo 2, 28029-Madrid, Spain. Email: silvia.arribas@uam.es

It is well established that chronic hypertension is associated with structural changes in the resistance vasculature (for reviews see Schiffrin, 1992; Heagerty *et al.* 1993; Mulvany, 2002). These alterations, known as 'remodelling' are now considered to be a complex process that might involve an increase (hypertrophy), a decrease (hypotrophy) or a rearrangement (eutrophy) of wall material (Mulvany *et al.* 1996; Mulvany, 2002). In the majority of models of hypertension studied, internal diameter is reduced and wall:lumen ratio is increased in small arteries if they are compared under equivalent biophysical conditions (for reviews see Schiffrin, 1992; Heagerty *et al.* 1993; Mulvany, 2002). Small arteries with internal diameters $< 500\ \mu$m have been shown to contribute substantially to precapillary resistance and might be defined as resistance arteries (Mulvany & Aalkjaer, 1990). The above-mentioned structural alteration has been termed 'inward' remodelling (Mulvany *et al.* 1996).

Vascular remodelling is also associated with altered mechanical properties (Intengan & Schiffrin, 2000). In most studies arterial distensibility is reduced in mesenteric resistance vessels (Intengan *et al.* 1999; Intengan & Schiffrin, 2000). It is known that vascular stiffness is greatly influenced by the extracellular matrix (Dobrin, 1978). The majority of studies on resistance arteries have focused on the alterations in collagen and, more recently, on non-fibrous extracellular matrix proteins and adhesion molecules (Intengan & Schiffrin, 2000). However, elastin is also an important determinant of arterial distensibility (Dobrin, 1978; Jacob *et al.* 2001). In large arteries, abnormalities in elastin content (Keeley & Alatawi, 1991) or structure (Boumaza *et al.* 2001; Cohuet *et al.* 2001) have been reported in several models of genetic hypertension. However, less attention has been paid to the role of elastin in resistance vessels and, to the best of our knowledge, there are no studies of elastin organisation in resistance

arteries in hypertension. Therefore, the aim of the present study was to analyse the role of elastin in the vascular remodelling and mechanical alterations of mesenteric resistance arteries (MRA) from SHR. Most studies of elastin structure have been performed with electron microscopy (Campbell & Roach, 1981; Roach & Song, 1988; Davis, 1995). Confocal microscopy offers a different approach for studying elastin organisation from a 3-dimensional (3D) point of view, without the distortions imposed by more classical histological techniques. This powerful tool allows examination of the internal elastic lamina (IEL) in whole-mount preparations of arteries fixed at physiological distension (Wong & Langille, 1996; Boumaza *et al.* 2001).

METHODS

Animals

Six-month-old male rats were obtained from the colonies of WKY and SHR rats (derived from the Charles River strains) inbred at the Animal House of Facultad de Medicina, Universidad Autónoma de Madrid. Systolic blood pressure (SBP) was measured in conscious rats by means of tail cuff plethysmography. Rats were anaesthetised with sodium pentobarbital (50 mg kg^{-1} I.P.) and killed by decapitation. The investigation conformed to the *Guide for the Care and Use of Laboratory Animals* published by the US National Institute of Health (NIH publication No. 85-23, revised in 1996) and with guidelines set by Spanish legislation regarding the use of experimental animals (RD 223/1988).

Preparation of arteries

The mesenteric bed was removed and placed in a dissecting dish containing modified Krebs Henseleit solution (KHS) at 4 °C; the KHS had the following composition (mM): 119 NaCl, 4.7 KCl, 2.5 $CaCl_2$, 24 $NaHCO_3$, 1.18 KH_2PO_4, 1.2 $MgSO_4$, 0.01 EDTA, 5.5 glucose. A third-order branch of mesenteric artery was isolated from the mesenteric bed and was carefully cleaned of surrounding tissue under a dissecting microscope.

Pressure myography

The structural and mechanical properties of MRA were studied with a pressure myograph (Danish Myo Tech, Model P100, J.P. Trading I/S, Aarhus, Denmark), as previously described (Coats & Hillier, 1999). Briefly, the vessel was placed on two glass microcannulae, secured with surgical nylon suture and vessel length was adjusted so that the vessel walls were parallel without stretch. Intraluminal pressure was then raised to 120 mmHg and the artery was unbuckled by adjusting the cannulae. The segment was then set to a pressure of 70 mmHg and allowed to equilibrate for 60 min at 37 °C in calcium-free KHS ($0Ca^{2+}$; omitting calcium and adding 10 mM EGTA) gassed with a mixture of 95 % O_2 and 5 % CO_2. Intraluminal pressure was reduced to 3 mmHg. A pressure–diameter curve was obtained by increasing intraluminal pressure in 20 mmHg steps between 20 and 120 mmHg. Internal and external diameters (D_{i0Ca} and D_{e0Ca}) were measured. Finally, the artery was set to 70 mmHg in $0Ca^{2+}$, pressure-fixed with 4 % paraformaldehyde (PFA, in 0.2 M phosphate buffer, pH 7.2–7.4) at 37 °C for 60 min and kept in 4 % PFA at 4 °C for confocal microscopy studies.

Calculation of structural and mechanical parameters

From internal and external diameter measurements in passive conditions the structural parameters wall thickness (WT), cross-sectional area (CSA) and wall:lumen ratio were calculated as follows:

$$\mathrm{WT} = (D_{e0Ca} - D_{i0Ca})/2,$$

$$\mathrm{CSA} = (\pi/4) \times (D_{e0Ca}{}^2 - D_{i0Ca}{}^2),$$

$$\mathrm{Wall/lumen} = (D_{e0Ca} - D_{i0Ca})/ 2D_{i0Ca}.$$

The following mechanical parameters were calculated according to the method of Baumbach & Heistad (1989).

$$\text{Incremental distensibility} = \Delta D_{i0Ca} /(D_{i0Ca} \times \Delta P) \times 100.$$

Incremental distensibility represents the percentage of change of the arterial internal diameter (D_{i0Ca}) for each 1 mmHg change in intraluminal pressure (P).

$$\text{Circumferential wall strain } (\epsilon) = (D_{i0Ca} - D_{00Ca})/D_{00Ca},$$

where D_{00Ca} is the diameter at 3 mmHg and D_{i0Ca} is the observed internal diameter for a given intravascular pressure, both measured under relaxed conditions.

$$\text{Circumferential wall stress } (\sigma) = (P \times D_{i0Ca})/(2\mathrm{WT}),$$

where P is the intraluminar pressure (1 mmHg = 133.4 N m^{-2}) and WT is wall thickness at each intraluminar pressure in $0Ca^{2+}$.

Arterial stiffness independent of geometry is determined by the Young's elastic modulus (E = stress/strain). The stress–strain relationship is non-linear. Therefore, it is more appropriate to obtain a tangential or incremental elastic modulus (E_{inc}) by determining the slope of the stress–strain curve ($E_{inc} = \delta\sigma/\delta\epsilon$) (Dobrin, 1978). E_{inc} was obtained by fitting the stress–strain data from each animal to an exponential curve using the equation:

$$\sigma = \sigma_{orig} \exp(\beta\epsilon),$$

where σ_{orig} is the stress at the original diameter (diameter at 3 mmHg). Taking derivatives on the above equation we see that $E_{inc} = \beta\sigma$. For a given σ value, E_{inc} is directly proportional to β. An increase in β implies an increase in E_{inc}, which means an increase in stiffness.

Growth index (GI) was calculated according to the method of Heagerty *et al.* (1993).

$$\mathrm{GI} = 100 \times (\mathrm{CSA_h} - \mathrm{CSA_n})/\mathrm{CSA_n},$$

where $\mathrm{CSA_n}$ and $\mathrm{CSA_h}$ are media cross-sectional areas of normotensive and hypertensive vessels, respectively.

Confocal microscopy study of elastin content and organization

The study of the content and organisation of elastin in MRA from SHR and WKY rats was performed, using a fluorescence confocal microscope, in maximally relaxed intact segments pressure-fixed at 70 mmHg. Elastin has autofluorescent properties, being excited at 488 nm; emitted fluorescence can be detected at 500–560 nm wavelength (Wong & Langille, 1996; Boumaza *et al.* 2001). Although much weaker, collagen can also show autofluorescence in the same wavelength range (Lee *et al.* 1993). In aorta and carotid arteries from several species it has been shown previously that 0.1 M NaOH at 75 °C for 1, 2 or 5 h is able to digest all non-elastin components (Potter & Roach, 1983; Roach & Song, 1988; Wong & Langille,

1996). Therefore, to determine if the source of autofluorescence was elastin, a group of experiments was performed in which the arteries were incubated for 0.5 or 1 h in 0.1 M NaOH at 75°C before examination with confocal microscopy.

Intact arterial segments were mounted in Fluoroguard (glycerol:antifade; Biorad) on slides with a small well (400 μm depth) made of silicon spacers to avoid vessel compression. The artery was visualised with a Leica TCS SP2 confocal system fitted with an inverted microscope and argon and helio-neon laser sources. Serial optical sections (stacks of images) from the adventitia to the lumen (z step= 0.5 μm) were captured with a × 63 oil objective (NA 1.3) and × 100 oil objective (NA 1.4), using the 488-nm line of the confocal microscope. A minimum of two stacks of images of different regions were captured in each arterial segment. All the images were taken under identical conditions of laser intensity, brightness and contrast.

Quantitative analysis of fluorescence intensity and fenestrae size

Quantitative analysis was performed with MetaMorph Image analysis software (Universal Imaging Corporation). From each stack of serial images, individual projections of the adventitia, external elastic lamina (EEL) and IEL were reconstructed and IEL thickness was measured.

From IEL projections several measurements were obtained as follows. The fluorescence intensity of elastin (average fluorescent intensity per pixel) was measured in several regions (minimum of 5) of the projection and averaged. Knowing that the concentration of elastin has a linear relationship with fluorescence intensity (Blomfield & Farrar, 1969), we can assume that the fluorescent signal in the projection is directly proportional to the concentration of elastin in a given pixel. An estimate of the amount of elastin in the IEL was made taking into account the average fluorescence intensity per pixel, IEL thickness and luminal surface area occupied by the IEL in a 1 mm length segment.

IEL projections were segmented and binary images were obtained. In these images, the relative area occupied by elastin *versus* fenestrae, as well as the number and size of fenestrae, were measured. The volume occupied by the IEL (including elastin and fenestrae) was calculated in every artery from the luminal surface area of a 1 mm length segment and the IEL thickness. The volume occupied by the elastin in the IEL was quantified in a similar way, taking into account the relative area occupied by elastin in the image.

Elastin degradation experiments

To determine the contribution of elastin to structural and mechanical properties of MRA we performed a set of paired experiments before and after incubation with elastase (pancreatopeptidase E, EC.3.4.21.36, porcine pancreas, Sigma).

To determine the optimum concentration of the enzyme preliminary experiments were performed in WKY MRA. MRA segments were incubated with 0.5, 0.25, 0.125 or 0.062 mg ml^{-1} elastase dissolved in KHS for 15, 30 or 60 min at 37°C. Thereafter, the segments were visualised with confocal microscopy, as previously described, to assess the degree of elastin degradation. The effect of 0Ca^{2+} medium on elastin degradation by elastase was also tested in order to design the pressure myography protocols. Based on these preliminary experiments (see Results) the following conditions were chosen: 0.065 mg ml^{-1} elastase dissolved in KHS with calcium (2.5 mM) and 60 min incubation time at 37°C.

MRA segments from WKY and SHR were mounted on a pressure myograph, set to a pressure of 70 mmHg and allowed to equilibrate for 30 min in gassed KHS at 37°C. Thereafter, the segment was incubated for 30 min with 0Ca^{2+}. As previously described, a first pressure–diameter curve (20–140 mmHg) was obtained and diameters were measured. The segment was then set to 3 mmHg, allowed to equilibrate 15 min in gassed KHS and incubated for 60 min with elastase 0.065 mg ml^{-1} in KHS at this pressure. After a 15 min washout period with 0Ca^{2+}, a second pressure–diameter curve was obtained. The segment was then set to 70 mmHg, pressure fixed with 4% PFA and analysed with confocal microscopy.

Statistical analysis

Results are expressed as means ± S.E.M. and n denotes the number of animals used in each experiment. The dependency of either vascular structure or mechanics on rat strain/elastase incubation and intraluminal pressure was studied by a two-way analysis of variance (ANOVA) within the framework of the general linear model approach (Littell *et al.* 1991). For specific two-means comparisons Student's t test was used. Statistical analysis was carried out with the SAS/STAT statistical package (SAS Institute Inc. Cary, NC, USA, 2000). A value of $P < 0.05$ was considered significant.

RESULTS

Body weight (BW) was similar between strains (BW_{SHR} = 382 ± 7 g, n = 15; BW_{WKY} = 374 ± 11 g, n = 15). SBP was significantly larger in SHR compared with WKY rats (SBP_{SHR} = 234 ± 9 mmHg; SBP_{WKY} = 159 ± 6 mmHg; $P < 0.01$).

Vascular structure and mechanics

Figure 1 shows the morphology of MRA under fully relaxed conditions (Ca^{2+}-free extracellular conditions). Lumen diameter was significantly smaller in MRA from hypertensive rats (Fig. 1*A*). Wall thickness was significantly increased in mesenteric arteries from SHR (at 60 mmHg, WKY WT = 30.2 ± 0.9 μm and SHR WT = 35.2 ± 1.5 μm; $P < 0.05$), but CSA was similar between strains (Fig. 1*B*). The growth index of SHR vessels was 0.3%. The wall:lumen ratio was significantly larger in mesenteric vessels from SHR (Fig. 1*C*).

Media stress was significantly smaller in SHR than in WKY (Fig. 1*D*). Incremental distensibility at low pressure (< 40 mmHg) was significantly smaller in SHR than in WKY, while no such difference was found at higher pressures (Fig. 1*E*). SHR MRA showed increased stiffness, as shown by the leftward shift of the stress–strain relationship (Fig. 1*F*) and the significantly larger value of β (WKY β = 3.9 ± 0.1; SHR β = 4.5 ± 0.2; $P < 0.05$).

Elastin autofluorescence

MRA segments showed autofluorescence in the adventitia and in the IEL. This was shown to be due to elastin since MRA digested with 0.1 M NaOH for up to 1 h showed similar

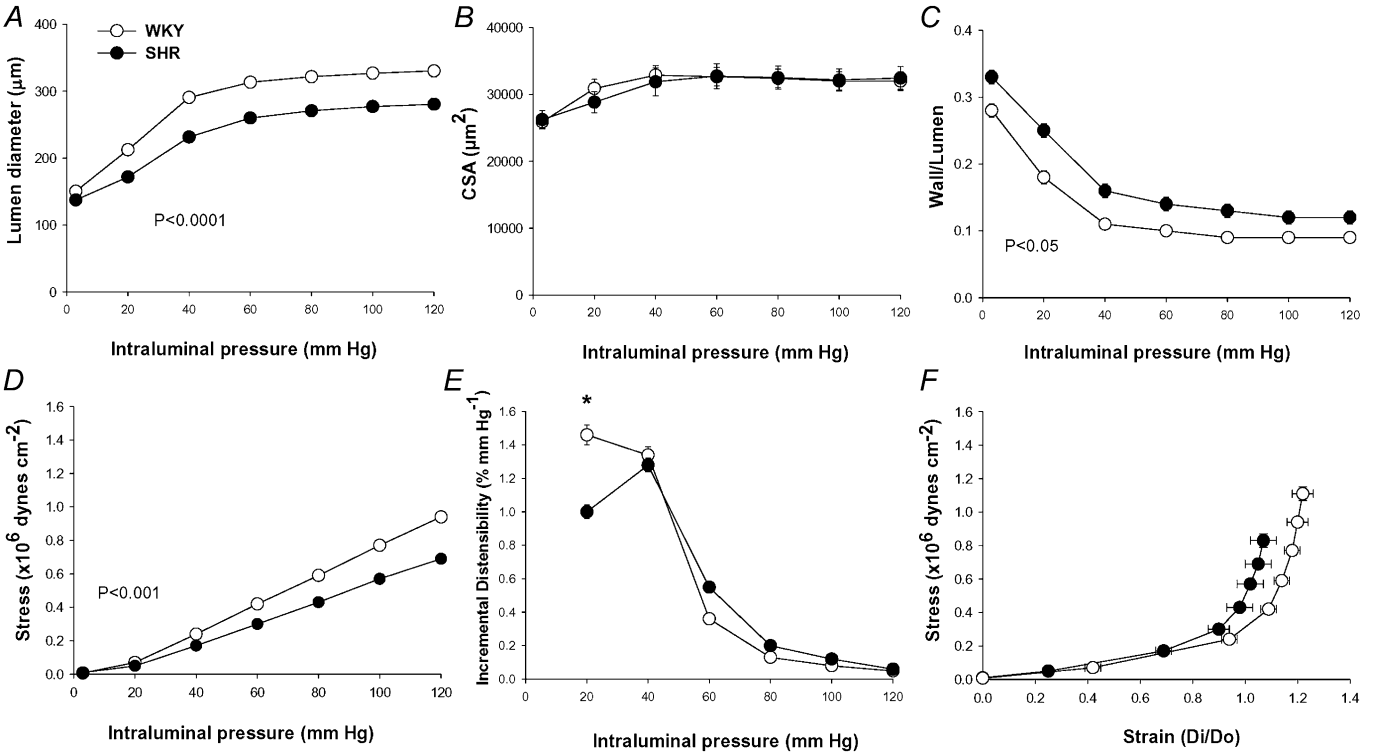

Figure 1. Comparison of structural and mechanical parameters in mesenteric resistance arteries (MRA) from WKY and SHR

Lumen diameter–intraluminal pressure (*A*), cross-sectional area (CSA)–intraluminal pressure (*B*) and wall:lumen ratio–intraluminal pressure (*C*), stress–intraluminal pressure (*D*), incremental distensibility–intraluminal pressure (*E*) and stress–strain (*F*) curves in fully relaxed MRA from SHR and WKY rats. Data are expressed as means ± S.E.M. Number of animals = 7–10. *P* values indicate statistical difference between strains by two-way (rat strain–pressure) ANOVA with repeated measures on the pressure factor. * $P < 0.05$ SHR *vs.* WKY at 20 mmHg by Student's unpaired *t* test.

autofluorescence levels and structure to control segments (Fig. 2). In addition, incubation with elastase caused a time- and concentration-dependent degradation of elastin. All incubation times and concentrations of elastase tested removed elastin in the adventitial side (data not shown). However, short incubation periods (15 and 30 min) did not affect IEL integrity, even at the highest concentration used (data not shown). Incubation with elastase for 60 min

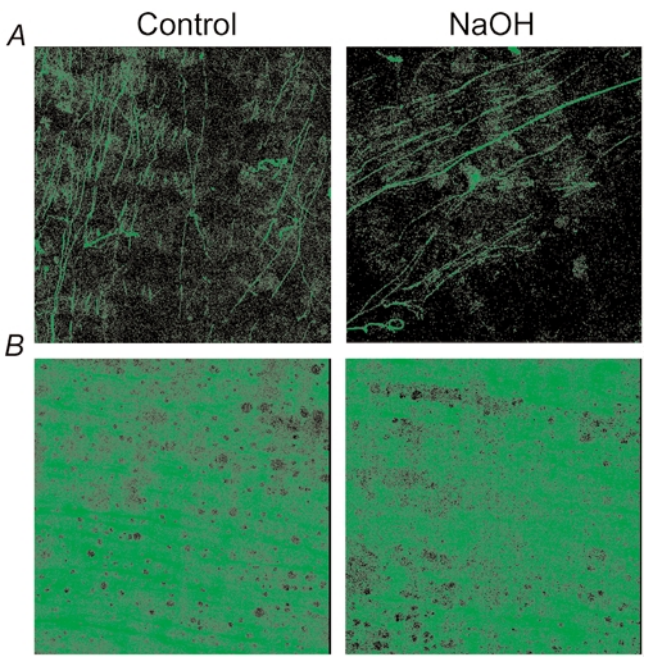

Figure 2. Confocal projections showing the effect of NaOH on elastin autofluorescence of mesenteric resistance arteries (MRA)

MRA segments from WKY rat were incubated for 60 min with 0.1 M NaOH at 75 °C and mounted intact on a slide. Projections were obtained of serial optical sections of the adventitia (*A*) and internal elastic lamina (*B*) captured with a fluorescence confocal microscope (× 63 oil immersion objective). Image size 238 × 238 μm.

Table 1. Characteristics of internal elastic lamina in pressurised segments of mesenteric resistance arteries from Wistar Kyoto and spontaneously hypertensive rats

	WKY	SHR
IEL thickness (μm)	2.50 ± 0.1	2.45 ± 0.2
No. of fenestrae per image	129 ± 10	125 ± 8
Total no. of fenestrae	3997 ± 566	2639 ± 316
Fenestra area (μm^2)	36.6 ± 5.0	12.4 ± 1*
Relative area of elastin per image	0.55 ± 0.04	0.83 ± 0.02*
IEL volume per artery (mm^3)	0.0028 ± 0.0001	0.0024 ± 0.0001*
Volume of elastin per artery (mm^3)	0.0016 ± 0.0001	0.0020 ± 0.0001*
Intensity per pixel	47.9 ± 7.1	52.9 ± 4.7
Total fluorescence (× 10^6) (intensity per pixel × volume)	1316 ± 166	1268 ± 114

Data are expressed as means ± S.E.M.; WKY, Wistar Kyoto rats; SHR, spontaneously hypertensive rats; IEL, internal elastic lamina; *P <0.01, SHR *vs.* WKY by Student's unpaired t test.

modified IEL structure in a concentration-dependent fashion: 0.5 mg ml^{-1} (data not shown) or 0.25 mg ml^{-1} elastase completely removed autofluorescence from the artery, 0.125 mg ml^{-1} and 0.062 mg ml^{-1} degraded the structure of the IEL, the effect of 0.125 mg ml^{-1} being larger (Fig. 3). In both strains, elastin degradation did not occur if elastase incubation took place in calcium-free medium (Fig. 4).

Detailed analysis of confocal projections of different parts of the arterial wall showed that in WKY and SHR MRA autofluorescence in the adventitia comprised a distinct EEL composed of fibres forming a clear network separating the adventitial layer from the media plus a set of isolated fibres outside this (Fig. 5). No fluorescence was observed in the medial layer (data not shown). The IEL had the clearly

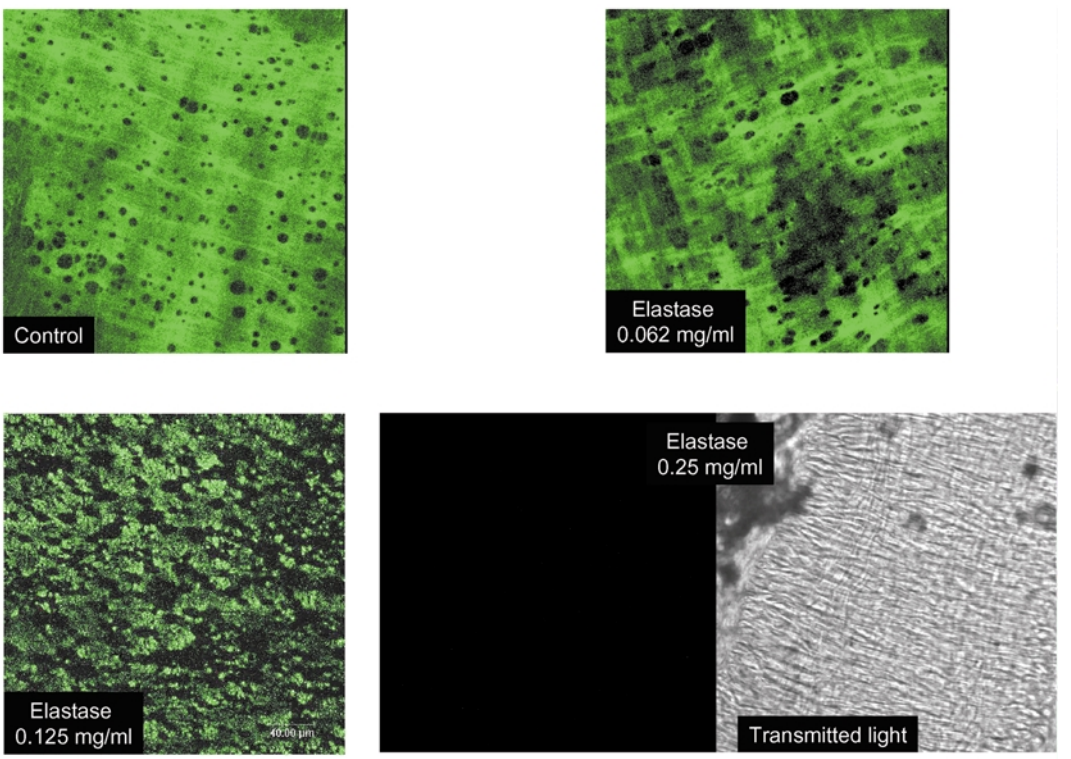

Figure 3. Confocal projections showing the effect of different concentrations of elastase on internal elastic lamina autofluorescence of mesenteric resistance arteries (MRA)

MRA segments from WKY rats were pressurised at 70 mmHg, incubated for 60 min with 0.062, 0.125 or 0.25 mg ml^{-1} elastase at 37 °C, fixed at 70 mmHg and mounted intact on slides. Projections were obtained of serial optical sections of internal elastic lamina captured with a fluorescence confocal microscope (× 63 oil immersion objective lens). Control, without elastase. Right bottom panels show a confocal projection of the internal elastic lamina without fluorescence and the corresponding transmitted light image. Image size 238 × 238 μm.

Journal of Physiology

Table 2. Effect of elastase on wall thickness and β values of mesenteric resistance arteries from Wistar Kyoto and spontaneously hypertensive rats measured under fully relaxed conditions

	Before elastase		After elastase	
	WKY	SHR	WKY	SHR
WT (μm)	29.3 ± 3.1	37.6 ± 1.9*	26.2 ± 2.9	25.7 ± 1.7†
β	4.2 ± 0.1	4.8 ± 0.19*	30.31 ± 4.3†	30.94 ± 2.5†

Data are expressed as means ± S.E.M.; WKY, Wistar Kyoto rats; SHR, spontaneously hypertensive rats; WT, wall thickness measured at 60 mmHg; *$P < 0.05$, SHR *vs.* WKY by Student's unpaired *t* test, †$P < 0.01$, after *vs.* before elastase by Student's paired *t* test, n=7.

organised structure of a compact fenestrated sheet in both strains (Fig. 5).

IEL thickness and the number of fenestrae per image, as well as total fenestrae number per surface area were similar between strains (Table 1). In WKY, large fenestrae were predominant (Fig. 5) and the mean fenestrae area was significantly larger (Table 1). The relative area occupied by elastin per image was significantly larger in SHR when compared to WKY (Table 1). As a result, the volume occupied by the elastin compartment within the IEL was

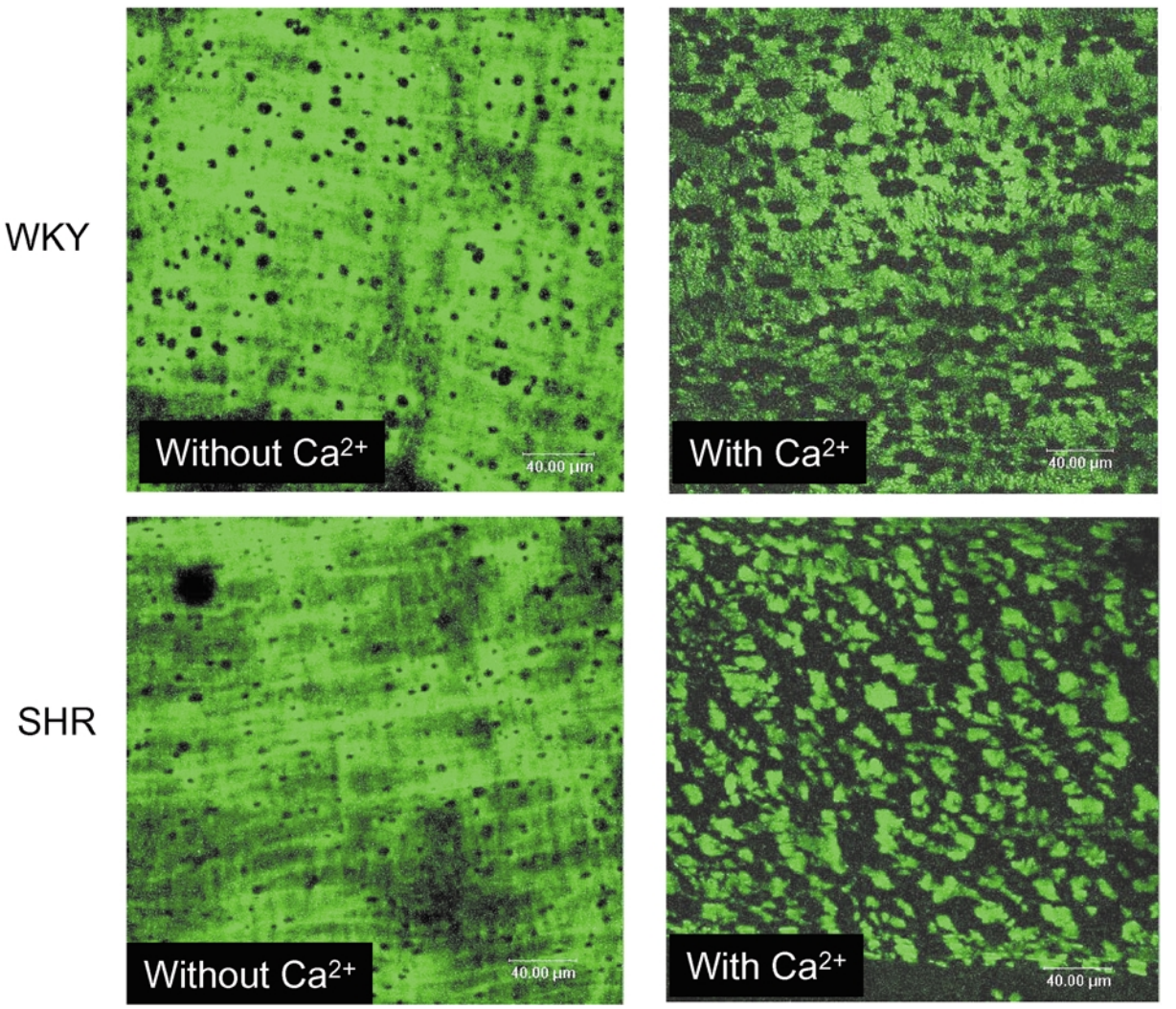

Figure 4. Confocal projections showing the effect calcium on internal elastic lamina degradation by elastase of SHR and WKY mesenteric resistance arteries (MRA)

MRA segments from SHR and WKY rats were pressurised at 70 mmHg, incubated for 60 min with 0.125 mg ml^{-1} elastase at 37 °C in the presence or absence of calcium, fixed at 70 mmHg and mounted intact on slides. Projections were obtained of serial optical sections of internal elastic lamina captured with a fluorescence confocal microscope (× 63 oil immersion objective lens). Image size 238 × 238 μm.

Journal of Physiology

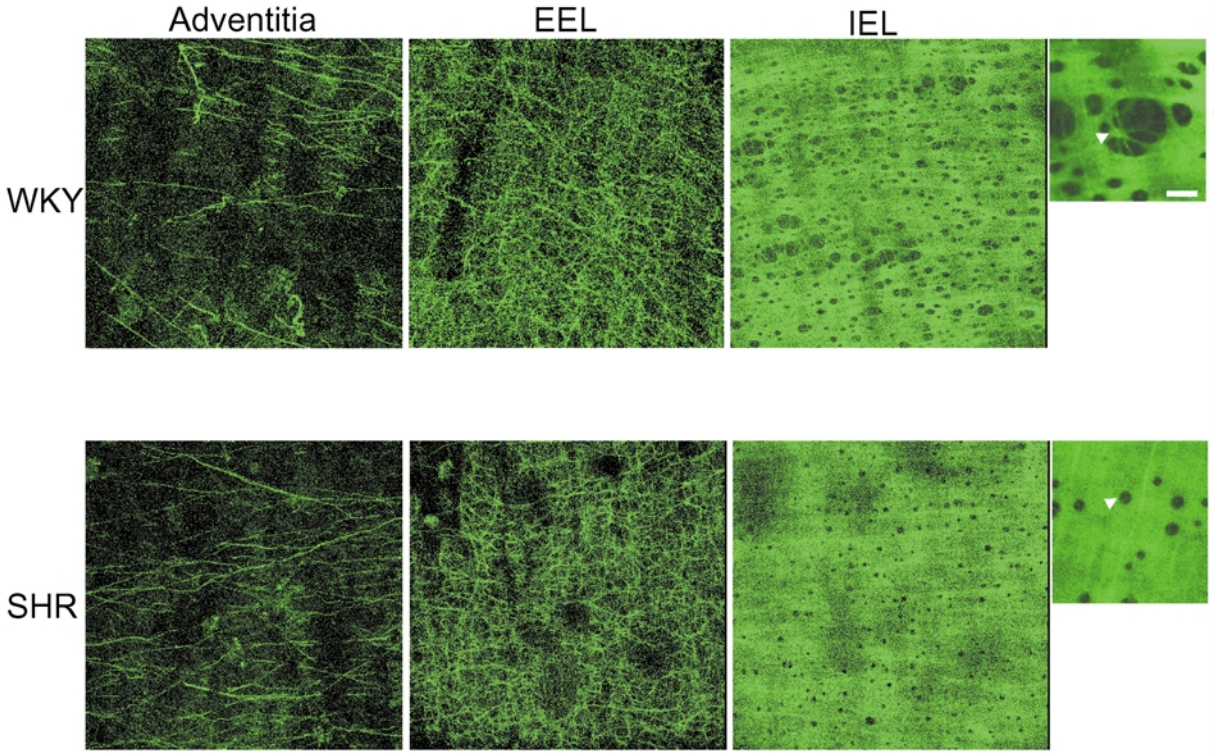

Figure 5. Confocal projections of the adventitia, external elastic lamina and internal elastic lamina from WKY and SHR mesenteric resistance arteries (MRA)

MRA segments were pressure-fixed at 70 mmHg and mounted intact on a slide. Projections were obtained from serial optical sections captured with a fluorescence confocal microscope (×63 oil immersion objective lens). Images show autofluorescence of isolated fibres in the adventitia, external elastic lamina (EEL) and internal elastic lamina (IEL) from WKY and SHR. Image size 238 × 238 μm. Small panels show a detail of IEL and fenestrae size (arrowheads) at higher magnification (× 63 oil, zoom 4, bar = 8 μm).

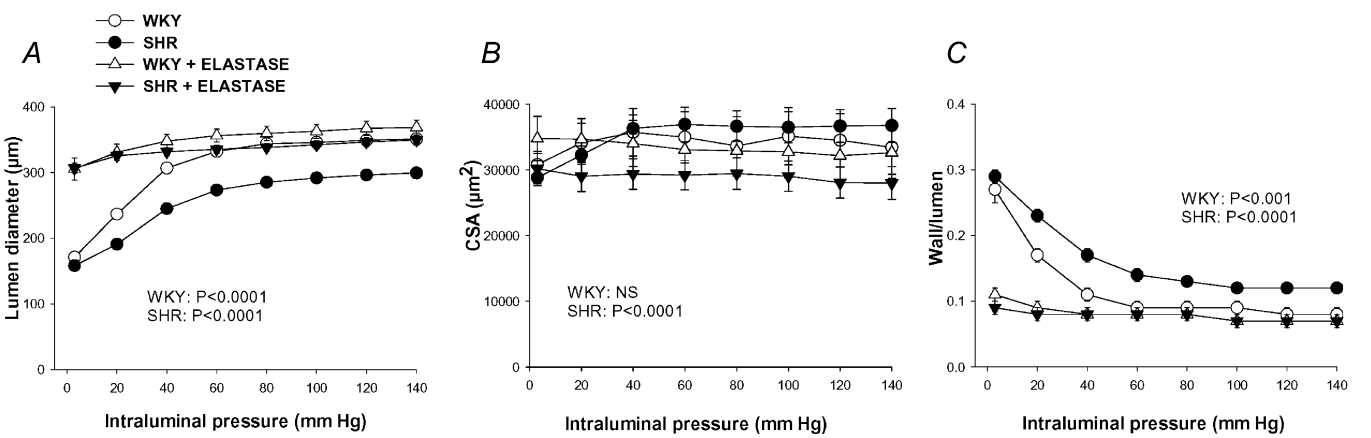

Figure 6. Effect of incubation with elastase on structural parameters of mesenteric resistance arteries (MRA) from WKY and SHR

Lumen diameter, cross-sectional area (CSA) and wall:lumen ratio were measured in MRA segments pressurised at several distending pressures before and after incubation with 0.062 mg ml^{-1} elastase for 60 min at 37 °C (paired experiments). Data are expressed as means ± S.E.M. Number of animals = 7–8. *P* values indicate statistical differences after elastase incubation for each rat strain; two-way (elastase incubation, pressure) ANOVA with repeated measures on both factors.

significantly larger in SHR, despite the fact that the total volume of the IEL (elastin plus fenestrae) was, in fact, smaller in SHR (Table 1).

Average fluorescence intensity per pixel was not significantly different between strains, so there was no evidence for a difference in the total amount of elastin in a 1 mm length of artery (Table 1).

Effect of elastase on vascular structure and mechanics

To study the effect of elastase on vascular structure and mechanical properties we used the lowest concentration that produced IEL degradation (0.062 mg ml^{-1}) incubated in KHS with calcium for 60 min.

Figure 6 shows the structural parameters – lumen diameter, CSA and wall : lumen ratio – from SHR and WKY MRA at different distending pressures, before and after the incubation with elastase. Elastase increased lumen diameter and decreased the wall : lumen ratio in both rat strains and reduced wall thickness and CSA only in SHR (Fig. 6, Table 2). In addition, elastase eliminated all the differences in the structural parameters observed between strains (Table 2, Fig. 6). With respect to vascular mechanics, elastase increased wall stress, reduced distensibility at pressures < 80 mmHg and increased vessel stiffness as shown by the significantly larger value of β and the leftward shift of the stress–strain curves in both strains (Table 2, Fig. 7). Elastase also abolished the differences in all mechanical parameters between strains (Fig. 7).

DISCUSSION

The present study describes for the first time, the overriding role of elastin in determining vascular dimensions and mechanical properties in a resistance artery. In addition, we describe 'remodelling' of the IEL in intact mesenteric resistance vessels in hypertension, which could participate in the increased vascular stiffness observed in these arteries. We suggest that elastin re-organization in the IEL could contribute to MRA remodelling in SHR and provide a potential pathophysiological basis for human hypertension.

Structural and mechanical alterations in MRA from SHR

MRA from SHR showed eutrophic inward remodelling compared with WKY since CSA was not significantly different yet the lumen was smaller. Previous studies of the mesenteric resistance vasculature from SHR have also shown eutrophic remodelling, although with a small contribution of growth that was not found in our study (Mulvany *et al.* 1985; Deng & Schiffrin 1992; Heagerty *et al.* 1993; Intengan *et al.* 1999). This small difference could be attributed to inter-strain variability or slight variations in MRA sizes.

Inward remodelling is believed to contribute to the increase in total peripheral resistance and thus to perpetuation of hypertension irrespective of tissue demand for blood flow. Small arteries have been estimated to operate at close to half of SBP in the rat (Halpern & Kelly, 1991). According to measurements of SBP in our WKY and SHR rats (159 and 234 mmHg), this would give comparative values of 80 and 115 mmHg, respectively. Comparing SHR and WKY vessel diameters at these physiological pressures (Fig. 1), the SHR arteries still maintain a smaller calibre than vessels from WKY rats.

Vascular remodelling in hypertension is known to be associated with altered mechanical properties (Intengan & Schiffrin, 2000). Stiffness was increased in MRA from SHR, as shown by larger β values. Similar results have been observed previously in SHR MRA (Laurant *et al.* 1997; Intengan *et al.* 1999), whereas no differences in intrinsic elastic properties were found in MRA from Dahl salt-sensitive (Intengan & Schiffrin, 1998) and mRen-2 transgenic rats (Dunn & Gardiner, 1997).

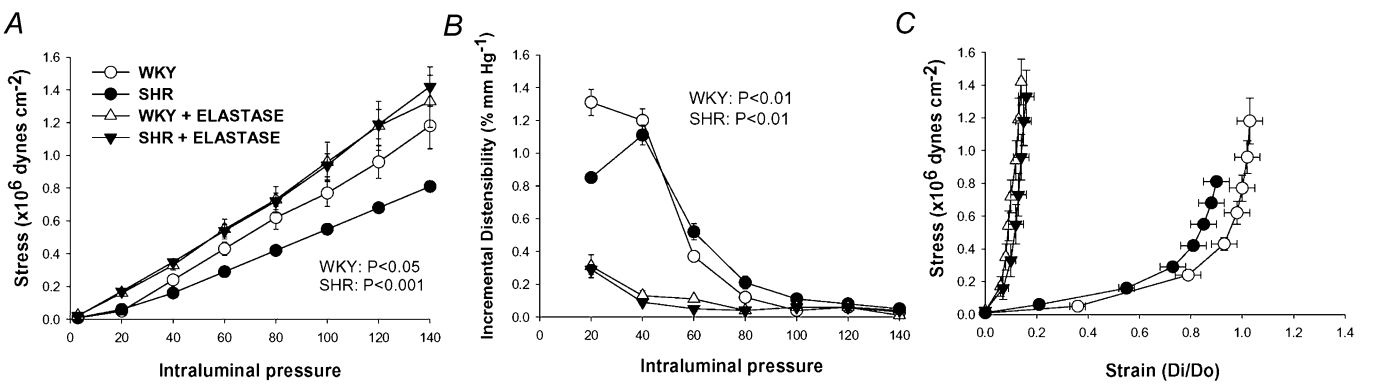

Figure 7. Effect of incubation with elastase on mechanical parameters of mesenteric resistance arteries (MRA) from WKY and SHR

Stress, strain and incremental distensibility were calculated at several distending pressures before and after incubation with 0.062 mg ml^{-1} elastase for 60 min at 37 °C (paired experiments). Number of animals = 7–8. *P* values indicate statistical differences after elastase incubation for each rat strain; two-way (elastase incubation, pressure) ANOVA with repeated measures on both factors.

Enhanced vascular stiffness in hypertension has been generally attributed to an increase in collagen content (Laurant *et al.* 1997; Intengan et al. 1999). Elastin is also considered an important determinant of arterial wall mechanical properties, and essential for vascular structural integrity and function (Dobrin, 1978; Keeley *et al.*, 1991; Jacob *et al.* 2001). However, the contribution of elastin to vascular mechanics and vessel structure has not been thoroughly studied in small arteries, probably due to the fact that these vessels contain a low proportion of elastin, compared with large arteries.

Role of elastin in MRA structure and mechanical properties

The present data provide clear evidence of the role of elastin in gross vascular structure and mechanical properties in resistance arteries. Firstly, we have demonstrated that elastin is an important element for MRA dimensions. The dramatic elastase-induced increase in lumen diameter at low pressures indicates that the conformation of elastin might be an essential determinant of lumen size and suggests that the other structures of the vascular wall, including smooth muscle and endothelium, passively adopt conformations dictated by elastin.

Secondly, our results also demonstrate that, despite the fact that resistance arteries have a small proportion of elastin, this protein plays an important role in vascular mechanics in these vessels. This is supported by the fact that elastin degradation by elastase induced a very large reduction (60–75 %) of MRA distensibility at low pressures, when elastin is known to contribute to vascular mechanics (Dobrin, 1978). In large arteries, it has been demonstrated that the first part of the stress–strain curve (low intravascular pressures) reflects the behaviour of gradually stretching elastin and the steeper part of the curve (high intraluminal pressures) reflects the stiffness of extended elastin with some contribution from stretched collagen fibres (Dobrin, 1978). The importance of elastin in MRA mechanical properties is also demonstrated by the spectacular increase in vessel stiffness after elastase incubation (6-fold increase in β value).

Role of elastin in MRA structural and mechanical alterations

Over the past two decades, there has been extensive research into vascular remodelling in hypertension and the different mechanisms and vascular elements involved in the process (Schiffrin, 1992; Heagerty *et al.* 1993; Mulvany, 2002). Changes in the expression and/or topographic localization of extracellular matrix components have been suggested to play a role in modulating the structure of the resistance vasculature in hypertension (Intengan & Schiffrin, 2000). The present data appear to represent an important new aspect of vascular remodelling, revealing for the first time the key role of elastin as a determinant of vascular structural alterations in hypertension. This is demonstrated by the fact that the well-known features of inward eutrophic remodelling – reduced lumen, increased wall thickness and wall:lumen ratio – were abolished by elastin degradation by elastase in pressurised MRA.

With the aid of confocal microscopy and elastin's autofluorescent properties we have investigated the possible changes in the content and/or organisation of elastin in resistance vessels from hypertensive rats that could participate in the observed inward remodelling of MRA. In physiological conditions, elastin is an extremely stable protein with a negligible turnover (Keeley & Alatawi, 1991). However, increases in elastin content (Keeley & Alatawi, 1991; Keeley *et al.* 1991) and changes in organisation (Boumaza *et al.* 2001) have been reported in large arteries in hypertensive animals. We found no difference in the total amount of elastin in the IEL (estimated from fluorescence intensity values and volumes of IEL) between strains. What was striking was the re-organisation of this elastin within the IEL. Over the total envelope of the IEL layer, elastin was distributed in a quite different way in the two rat strains. In the SHR, it was arranged to form dramatically smaller fenestrae, which had, however, a similar spacing, as shown by the similar number of fenestrae per surface area, to WKY. Since the diameter of the artery is smaller in SHR, the overall volume of IEL (with holes) is less in the hypertensive strain. However, calculation of the volume of the elastin component (excluding holes) shows it to be greater in SHR. Thus, when viewed in three dimensions, there is seen to be a eutrophic remodelling of the IEL that allows a smaller diameter and narrower mesh IEL. This implies a change in the matrix molecules responsible for arrangement of the elastin rather than a change in elastin synthesis *per se*. Similar changes in IEL 3D-structure without any modification in elastin content have been found in SHR and SHR-SP rat carotid arteries (Boumaza *et al.* 2001; Cohuet *et al.* 2001). It has been shown that the stress in the vicinity of fenestrae is several times higher than the average stress (Langille, 1991). It is therefore possible that the remodelling of the IEL together with the increased wall thickness in SHR vessels could contribute to a reduction in wall stress in response to a higher level of pressure. This is also supported by the fact that after elastin degradation by elastase, wall stress was significantly increased and the difference between WKY and SHR was abolished.

The present results demonstrate that elastin participates in the altered mechanical properties of MRA from the hypertensive strain. This is supported by the fact that the differences between WKY and SHR in incremental distensibility and stiffness were completely abolished after elastase incubation. Our data also demonstrate that it is not the amount of elastin, but the way that it is organised to form the IEL that dictates the mechanical alterations in

MRA from SHR. Smaller fenestrae are likely to make the IEL structure stiffer, providing a less distensible skeleton in SHR small vessels. We suggest that the alteration in the organisation of elastin, possibly together with the reported increase in collagen content (Laurant *et al.* 1997; Intengan *et al.* 1999), causes the increased stiffness in MRA from SHR. The reduction of fenestrae size could also have a functional implication: a decrease in the passage of blood-derived and endothelial factors through the IEL to the medial layer.

The difference in IEL structure between SHR and WKY cannot be discounted as a consequence rather than a cause of hypertension. However, since related abnormalities in intrinsic elastic properties have been found in MRA of SHR (Laurant *et al.* 1997; Intengan *et al.* 1999), but not in Dahl salt-sensitive (Intengan & Schiffrin, 1998) or mRen-2 transgenic rats (Dunn & Gardiner, 1997), this property seems likely to be genetic in this strain and, at least, a part of the explanation of its hypertension. Since changes in IEL structure without any modification in elastin content have been found in SHR and SHR-SP rat carotid arteries (Boumaza *et al.* 2001; Cohuet *et al.* 2001), it seems likely that the genetic defect is also present in the stroke-prone hypertensive strain.

Consideration of methods

The present study aimed to analyse the characteristics of vascular remodelling in small arteries under physiological conditions. As previously described (for reviews see Mulvany & Aalkjaer, 1990; Hughes & Bund, 2002), pressure myography is the method of choice for studying small vessel structure and function under close to physiological conditions. With the pressure myograph the vessel experiences a true transmural pressure and assumes a physiological shape (Halpern & Osol, 1986), which also allows detailed examination of 3D structure using confocal microscopy.

Evaluation of the role of elastin in hypertension has relied on determination of elastin content by biochemical methods, mainly in large vessels (for reviews see Keeley *et al.* 1991; Jacob *et al.* 2001). Smaller arteries contain a much lower proportion of elastin, which, together with their small size, makes it difficult to estimate elastin chemically. Elastin is autofluorescent, being excited by 488 nm wavelength and emitted fluorescence can be detected at 500–560 nm wavelength (Wong & Langille, 1996; Boumaza *et al.* 2001). We have used this property to determine the elastin content with confocal microscopy. In addition, this tool offers a unique approach to studying in detail possible alterations in elastin organisation in the different layers of the arterial wall, as it allows visualisation of intact arterial segments fixed at physiological pressure without the distortions imposed by more classical histological techniques (Arribas *et al.* 1999).

Hot alkali has been described as digesting all non-elastin components (Potter & Roach; 1983; Roach & Song, 1988; Wong & Langille, 1996). Using this method we demonstrated that the fluorescence we observed was due to elastin and not to other fluorescent components of the vascular wall such as collagen. This was further supported by the concentration-dependent reduction of autofluorescence by elastase. Pancreatic elastase belongs to the family of serine proteinases. It is unique among proteinases in having the ability to rapidly hydrolyse elastin (Balo & Banga, 1950). It is also able to hydrolyse various other proteins like haemoglobin, casein and fibrin (Shotton, 1970). We devised a protocol on the basis that it would digest the elastin of the IEL sufficiently to visibly degrade its continuous structure as shown by confocal microscopy. It has been demonstrated that macrophage elastase, a metallo-proteinase with elastolytic activity, is calcium dependent (Valentine & Fisher, 1984). Its activity can be inhibited by metal chelators such as EDTA (Valentine & Fisher, 1984; Gardi & Lungarella, 1987). Therefore, we tested the possibility that calcium-free medium would also affect pancreatic elastase performance. In fact our histological and functional experiments demonstrate that under calcium-free conditions the enzyme was ineffective at degrading elastin.

REFERENCES

Arribas SM, Daly CJ & McGrath JC (1999). Measurements of vascular remodeling by confocal microscopy. In *Methods in Enzymology. Confocal Microscopy,* vol. 307, ed. Conn PM, pp. 246–273. Academic Press, San Diego.

Balo J & Banga J (1950). The elastolytic activity of pancreatic extracts. *Biochem J* **46**, 384–387.

Baumbach GL & Heistad DD (1989). Remodeling of cerebral arterioles in chronic hypertension. *Hypertension* **13**, 968–972.

Blomfield J & Farrar JF (1969). The fluorescent properties of maturing arterial elastin. *Cardiovasc Res* **3**, 161–170.

Boumaza S, Arribas SM, Osborne-Pellegrin M, McGrath JC, Laurent S, Lacolley P & Challande P (2001). Fenestrations of the carotid internal elastic lamina and structural adaptation in stroke-prone spontaneously hypertensive rats. *Hypertension* **37**, 1101–1107.

Campbell GJ & Roach MR (1981). Fenestrations in the internal elastic lamina at bifurcations of human cerebral arteries. *Stroke* **12**, 489–496.

Coats P & Hillier C (1999). Determination of an optimal axial-length tension for the study of isolated resistance arteries on a pressure myograph. *Exp Physiol* **84**, 1085–1094.

Cohuet G, Challande P, Osborne-Pellegrin M, Arribas SM, Dominiczak A, Louis H, Laurent S & Lacolley P (2001). Mechanical strength of the isolated carotid artery in SHR. *Hypertension* **38**, 1167–1171.

Davis EC (1995). Elastic lamina growth in the developing mouse aorta. *J Histochem Cytochem* **43**, 1115–1123.

Deng LY & Schiffrin EL (1992). Effects of endothelin-1 and vasopressin on resistance arteries from spontaneously hypertensive rats. *Am J Hypertens* **5**, 817–822.

Dobrin PB (1978). Mechanical properties of arteries. *Physiol Rev* **58**, 397–460.

Dunn WR & Gardiner SM (1997). Differential alteration in vascular structure of resistance arteries isolated from the cerebral and mesenteric vascular beds of transgenic [(mRen-2)27], hypertensive rats. *Hypertension* **29**, 1140–1147.

Gardi C & Lungarella G (1987). Purification and partial characterization of elastase activity from rat alveolar and peritoneal macrophages. *Arch Biochem Biophys* **259**, 98–104.

Halpern W & Kelley M (1991). *In vitro* methodology for resistance arteries. *Blood Vessels* **28**, 245–251.

Halpern W & Osol G (1986). Resistance vessels in hypertension. In *Recent Advances in Arterial Diseases: Atherosclerosis, Hypertension and Vasospasm, Progress in Clinical and Biological Research,* vol. 219, ed. Tulenko TN & Cox RH, pp. 211–223. Alan R Liss, New York.

Heagerty AM, Aalkjaer C, Bund SJ, Korsgaard N & Mulvany MJ (1993). Small artery structure in hypertension. Dual processes of remodeling and growth. *Hypertension* **21**, 391–397.

Hughes JM & Bund SJ (2002). Arterial myogenic properties of the spontaneously hypertensive rat. *Exp Physiol* **87**, 527–534.

Intengan HD & Schiffrin EL (1998). Mechanical properties of mesenteric resistance arteries from Dahl salt-resistant and salt-sensitive rats: role of endothelin-1. *J Hypertens* **16**, 1907–1912.

Intengan HD & Schiffrin EL (2000). Structure and mechanical properties of resistance arteries in hypertension. Role of adhesion molecules and extracellular matrix determinants. *Hypertension* **36**, 312–318.

Intengan HD, Thibault G, Li JS & Schiffrin EL (1999). Resistance artery mechanics, structure, and extracellular components in spontaneously hypertensive rats. Effects of angiotensin receptor antagonism and converting enzyme inhibition. *Circulation* **100**, 2267–2275.

Jacob MP, Badier-Commander C, Fontaine V, Benazzoug Y, Feldman L & Michel JB (2001). Extracellular matrix remodeling in the vascular wall. *Pathol Biol* **49**, 326–332.

Keeley FW & Alatawi A (1991). Response of aortic elastin synthesis and accumulation to developing hypertension and the inhibitory effect of colchicine on this response. *Lab Invest* **64**, 499–507.

Keeley FW, Elmoselhi A & Leenen FHH (1991). Effects of antihypertensive drug classes on regression of connective tissue components of hypertension. *J Cardiovasc Pharmacol* **17** (suppl. 2), S64–S69.

Langille B (1991). Hemodynamic factors and vascular diseases. In *Cardiovascular Pathology,* ed. Silver MD, pp. 131–154. Churchill Livingstone, New York.

Laurant P, Touyz RM & Schiffrin EL (1997). Effect of pressurization on mechanical properties of mesenteric small arteries from spontaneously hypertensive rats. *J Vasc Res* **34**, 117–125.

Lee WK, Bell J, Kilpatrick E, Hayes M, Lindop GBM & Dominiczak MH (1993). Collagen-linked fluorescence in human atherosclerotic plaques. *Atherosclerosis* **98**, 219–227.

Littell RC, Freund RJ & Spector PC (1991). *SAS System for Linear Models,* ed. Cary NC. SAS Institute Inc., Cary, NC, USA.

Mulvany MJ (2002). Small artery remodeling in hypertension. *Curr Hypertens Rep* **4**, 49–55.

Mulvany MJ & Aalkjaer C (1990). Structure and function of small arteries. *Physiol Rev* **70**, 921–961.

Mulvany MJ, Baandrup U & Gundersen HJG (1985). Evidence for hyperplasia in mesenteric resistance vessels of spontaneously hypertensive rats using a 3-dimensional dissector. *Circ Res* **57**, 794–800.

Mulvany MJ, Baumbach GL, Aalkjaer C, Heagerty AM, Korsgaard N, Schiffrin EL & Heistad DD (1996). Vascular remodeling. *Hypertension* **28**, 505–506.

Potter RF & Roach MR (1983). Are enlarged fenestrations in the internal elastic lamina of the rabbit thoracic aorta associated with poststenotic dilatation? *Can J Physiol Pharmacol* **61**, 101–104.

Roach MR & Song SH (1988). Arterial elastin as seen with scanning electron microscopy: a review. *Scanning Microsc* **2**, 994–1004.

Schiffrin EL (1992). Reactivity of small blood vessels in hypertension: relation with structural changes. *Hypertension* **19** (suppl 2), 1–9.

Shotton DM (1970). Elastase. In *Methods in Enzymology,* vol. 19, ed. Colowick SP & Kaplan NO, pp. 113–140. Academic Press, New York.

Valentine R & Fisher GL (1984). Characteristics of bovine alveolar macrophage elastase. *J Leukoc Biol* **35**, 449–457.

Wong LCY & Langille BL (1996). Developmental remodeling of the internal elastic lamina of rabbit arteries. Effect of blood flow. *Circ Res* **78**, 799–805.

Acknowledgements

This work has been supported by the EU project VASCAN-2000 (QLG-CT-1999-00084); SAF 2000-1877-CE; SAF 2000-1924-CE; Ministerio de Ciencia y Tecnología (BFI 2001-0638), Acciones Integradas and Wellcome Trust. We are grateful to Diego Megías (Universidad Autónoma de Madrid) and Servei de Microscopia (Universitat Autónoma de Barcelona) for technical assistance with confocal microscopy. We also thank Mª Carmen Fernández Criado for the maintenance of the rat colonies at the Universidad Autónoma de Madrid.